nature chemical biology

BRIEF COMMUNICATION

PUBLISHED ONLINE: 6 MARCH 2011 | DOI: 10.1038/NCHEMBIO.538

Characterization of a selective inhibitor of the Parkinson's disease kinase LRRK2

Xianming Deng[1,2,7], Nicolas Dzamko[3,7], Alan Prescott[4], Paul Davies[3], Qingsong Liu[1,2], Qingkai Yang[5], Jiing-Dwan Lee[5], Matthew P Patricelli[6], Tyzoon K Nomanbhoy[6], Dario R Alessi[3]* & Nathanael S Gray[1,2]*

Mutations in leucine-rich repeat kinase 2 (LRRK2) are strongly associated with late-onset autosomal dominant Parkinson's disease. We employed a new, parallel, compound-centric approach to identify a potent and selective LRRK2 inhibitor, LRRK2-IN-1, and demonstrated that inhibition of LRRK2 induces dephosphorylation of Ser910 and Ser935 and accumulation of LRRK2 within aggregate structures. LRRK2-IN-1 will serve as a versatile tool to pharmacologically interrogate LRRK2 biology and study its role in Parkinson's disease.

Parkinson's disease is the second most common neurodegenerative disease in the world, with a prevalence of more than 1% after the age of 65 years[1]. Mutations in the leucine-rich repeat kinase-2 (*LRRK2*) gene were first linked to Parkinson's disease in 2004 (refs. 2,3), and extensive genetic, cellular and biochemical studies suggest that it is a key driver of the disease. Among the genes associated with Parkinson's disease, such as *parkin* and *PINK1*, *LRRK2* is unique because a missense mutation, G2019S, is frequently found in not only familial but also sporadic Parkinson's disease cases[4,5].

The most common and extensively characterized mutation, G2019S enhances kinase activity, suggesting that small-molecule LRRK2 kinase inhibitors may serve as potential therapeutic agents for the treatment of Parkinson's disease[6]. To date, only relatively nonspecific LRRK2 inhibitors have been reported, such as staurosporine[7,8], K252A[7,8], sunitinib[7–9], H-1152 (ref. 9) and GW5074 (ref. 10). Here we report the identification of a selective inhibitor of LRRK2 and demonstrate its ability both *in vitro* and *in vivo* to inhibit LRRK2.

In an effort to discover small molecules that can selectively inhibit LRRK2 kinase activity, we applied a novel, highly parallel, compound-centric strategy[11]. We screened a 300-member compound library designed to target the ATP-binding site against a panel of 442 diverse kinases using an *in vitro* ATP-site competition binding assay[12,13]. In contrast to the traditional, linear process of inhibitor discovery, this high-throughput kinase profiling enables rapid identification of compounds capable of selectively inhibiting LRRK2 and other kinases of interest. A series of 2-amino-5, 11-dimethyl-5H-benzo[e]pyrimido-[5,4-b][1,4]diazepin-6(11H)-one analogs emerged as potential LRRK2 inhibitors with strong binding affinities against both wild-type LRRK2 and LRRK2 mutant G2019S. LRRK2-IN-1 (**1**) was identified as a promising inhibitor after the synthesis of approximately 50 analogs guided by iterative rounds of synthesis and testing in biochemical and cellular assays (**Fig. 1a** and **Supplementary Methods**). LRRK2-IN-1 inhibits both wild-type and G2019S mutant LRRK2 kinase activity with IC_{50} (concentration required to inhibit 50% of enzyme activity) values of 13 nM and 6 nM (**Fig. 1b**), respectively, with 0.1 mM ATP in the assay. Consistent with LRRK2-IN-1 being an ATP-competitive inhibitor, the IC_{50} for G2019S mutant was increased when ATP was increased (**Supplementary Results**, **Supplementary Fig. 1**). Previous work identified a LRRK2[A2016T] mutant that is normally active but 32-fold less sensitive to H-1152 and 12-fold less sensitive to sunitinib[9]. Notably, LRRK2[A2016T] and LRRK2[A2016T + G2019S] mutants were ~400-fold more resistant to LRRK2-IN-1 (**Fig. 1b**). A molecular model of LRRK2-IN-1 binding to the ATP site of LRRK2 demonstrates that the A2016T mutation likely introduces an unfavorable steric interaction with the anthranilic acid phenyl group of LRRK2-IN-1 (**Supplementary Fig. 2**).

The kinase selectivity of LRRK2-IN-1 was comprehensively evaluated using three independent and complementary experimental approaches that in aggregate assessed the selectivity against >470

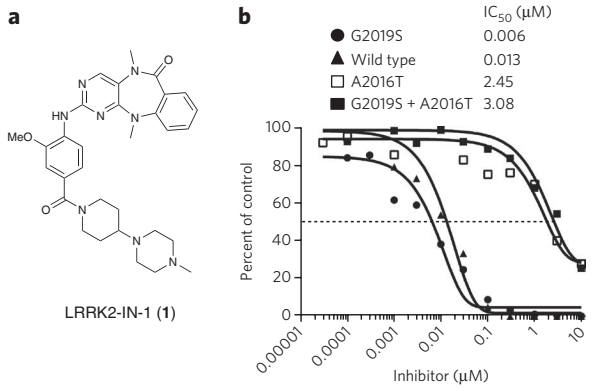

Figure 1 | Enzymatic activity of LRRK2-IN-1 and its selectivity. (**a**) Chemical structure of the LRRK2 inhibitor LRRK2-IN-1. (**b**) GST-LRRK2 (1,326–2,517), GST-LRRK2[G2019S] (1,326–2,527), GST-LRRK2 [A2016T] (1,326–2,517) and GST-LRRK2[A2016T + G2019S] (1,326–2,517) were assayed using 20 μM Nictide in the presence of 100 μM ATP with the indicated concentrations of LRRK2-IN-1. The results are presented as percentage of kinase activity relative to the DMSO-treated control. Results are averages of duplicate reactions with similar results obtained in at least one other experiment. The IC_{50} values, in μM, were derived from the graphs.

[1]Department of Cancer Biology, Dana-Farber Cancer Institute, Boston, Massachusetts, USA. [2]Department of Biological Chemistry & Molecular Pharmacology, Harvard Medical School, Boston, Massachusetts, USA. [3]MRC Protein Phosphorylation Unit, College of Life Sciences, University of Dundee, Dundee, Scotland. [4]Division of Cell Biology and Immunology, College of Life Sciences, University of Dundee, Dundee, Scotland. [5]Department of Immunology and Microbial Science, The Scripps Research Institute, La Jolla, California, USA. [6]ActivX Biosciences, La Jolla, California, USA. [7]These authors contributed equally to this work. *E-mail: nathanael_gray@dfci.harvard.edu or d.r.alessi@dundee.ac.uk

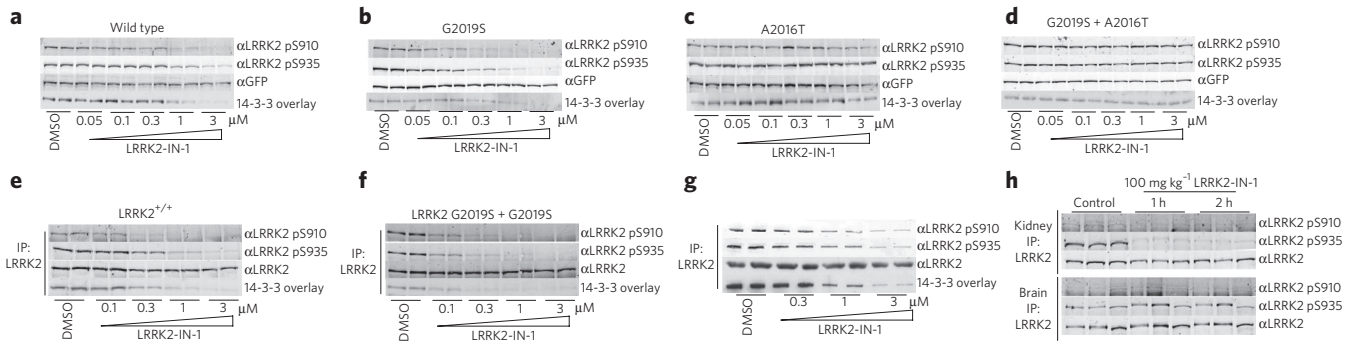

Figure 2 | LRRK2-IN-1 inhibits LRRK2 *in vivo*. (**a**) HEK 293 cells stably expressing wild-type GFP-LRRK2 were treated with DMSO or increasing concentrations of LRRK2-IN-1 for 90 min. Cell lysates were subjected to immunoblotting for detection of LRRK2 phosphorylated at Ser910 and Ser935 and for total GFP-LRRK2. 14-3-3 binding was measured by overlay assay after immunoprecipitation of LRRK2 with GFP-binder Sepharose. (**b**) As in **a** except HEK 293 cells stably expressing GFP-LRRK2[G2019S] were used. (**c**) As in **a** except HEK 293 cells stably expressing drug-resistant GFP-LRRK2 [A2016T] were used. (**d**) As in **a** except HEK 293 cells stably expressing drug-resistant GFP-LRRK2[A2016T + G2019S] cells were used. (**e**) Endogenous LRRK2 was immunoprecipitated (IP) with anti-LRRK2 100–500 from EBV immortalized human lymphoblastoid cells from a control subject and a Parkinson's disease patient homozygous for the LRRK2[G2019S] mutation. (**f**) After treatment of the cells with DMSO or the indicated concentrations of LRRK2-IN-1 for 90 min, immunoprecipitates were subjected to immunoblot analysis with the indicated antibody as well as 14-3-3 overlay for western analysis. Immunoprecipitations were performed in duplicate, and results are representative of at least two independent experiments. (**g**) As in **e** except that human SHSY5Y cells were used. (**h**) 100 mg kg^{-1} LRRK2-IN-1 was administered by intraperitoneal injection to wild-type mice (n = 3 per group). Tissues were collected and endogenous LRRK2 was immunoprecipitated and analyzed for Ser910 and Ser935 phosphorylation as above. Quantitation of immunoblots along with original images are available in **Supplementary Figure 11**.

kinases. These approaches included kinase-binding assays against a panel of 442 distinct kinases using the KINOME*scan* methodology (Ambit Biosciences)[12,13], standard radioactivity-based enzymatic assays against a panel of 105 kinases (Dundee profiling)[14] and activity-based proteomics against 260 kinases using the KiNativ technology (ActivX Biosciences)[15]. This analysis revealed that LRRK2-IN-1 possessed a selective profile (see **Supplementary Data Set**), inhibiting only 12 kinases among the Ambit 442 diverse kinases panel with a score of less than 10% of the DMSO control at a concentration of 10 μM. In the biochemical assays, LRRK2-IN-1 possessed an IC_{50} of 45 nM for inhibition of DCLK2 and had an IC_{50} of greater than 1 μM when evaluated in biochemical assays for AURKB, CHEK2, MKNK2, MYLK, NUAK1 and PLK1 (**Supplementary Table 1**). Biochemical assays are not available for MAPK7, DCLK1, PLK4, RPS6KA2 (Kin.Dom.2-C-terminal) and RPS6KA6 (Kin.Dom.2-C-terminal), therefore the dissociation constants (K_ds) were measured by KINOME*scan* binding assay (**Supplementary Table 1**). The selectivity score (S (3 μM)) for LRRK2-IN-1, calculated by dividing the number of kinases found to bind with a dissociation constant (K_d < 3 μM) by the total number of kinases tested, is 0.029 (13/442), which represents high selectivity (see **Supplementary Data Set**)[13]. Further exploration of the selectivity of LRRK2-IN-1 was performed by profiling directly against all kinases detectable in human peripheral blood mononuclear cells (hPBMC, 180 kinases) and mouse brain tissue (195 kinases) using KiNativ. This approach confirmed inhibition of LRRK2, DCLK1 and MAPK7 and supported >1 μM IC_{50}s for CHEK2, MYLK (smMLCK) and RPS6KA2. LRRK2-IN-1 was confirmed to inhibit MAPK7 with an EC_{50} (concentration required to inhibit autophosphorylation in cells by 50%) of 160 nM (**Supplementary Fig. 3**). We are unable to evaluate whether LRRK2-IN-1 inhibits LRRK1, as LRRK1 kinase activity cannot be measured under the same conditions employed for LRRK2 (**Supplementary Fig. 4**). Overall, the selectivity of LRRK2-IN-1 is sufficient for use as a tool compound for assessing the effects of LRRK2 inhibition in cellular systems.

LRRK2 binds to isoforms of 14-3-3 proteins, and this interaction depends on the phosphorylation of LRRK2 at Ser910 and Ser935 (ref. 16). Recent work suggested that inhibition of LRRK2 kinase activity stimulates an as-yet uncharacterized regulatory feedback loop promoting the release of 14-3-3 and dephosphorylation of LRRK2 at Ser910 and Ser935 (ref. 17). Indeed, LRRK2-IN-1 induced a dose-dependent inhibition of Ser910 and Ser935 phosphorylation accompanied by loss of 14-3-3 binding to both wild-type LRRK2 (**Fig. 2a**) and LRRK2[G2019S] stably transfected into HEK293 cells (**Fig. 2b**). Significant dephosphorylation of Ser910 and Ser935 was observed at 1–3 μM of LRRK2-IN-1 for wild-type LRRK2 and at slightly lower doses for LRRK2[G2019S] (**Fig. 2a**,**b**). Notably, LRRK2-IN-1 failed to induce dephosphorylation of Ser910 and Ser935 in the drug-resistant LRRK2[A2016T] (**Fig. 2c**) and LRRK2[A2016T + G2019S] (**Fig. 2d**) mutants, establishing that the effects of LRRK2-IN-1 on LRRK2 phosphorylation are indeed mediated via inhibition of LRRK2 kinase activity and are not because of off-target effects.

Near-maximal effects of 1 μM LRRK2-IN-1 on dephosphorylation of Ser910 and Ser935 and 14-3-3 binding to wild-type LRRK2 and LRRK2[G2019S] were observed within 15 min and sustained for at least 2 h (**Supplementary Fig. 5**). Phosphorylation of Ser910 and Ser935 and 14-3-3 binding were restored to near control levels within 2 h of removal of LRRK2-IN-1 from the tissue culture medium (**Supplementary Fig. 5**). We observed that kinase-inactive LRRK2 was phosphorylated at Ser910 and Ser935 at a slightly lower level than wild-type LRRK2, and treatment with LRRK2-IN-1 did not induce significant dephosphorylation of kinase-inactive LRRK2 (**Supplementary Fig. 6**).

We next examined the effect of LRRK2-IN-1 on endogenous LRRK2 phosphorylation and 14-3-3 binding in human lymphoblastoid cells derived from a control individual (**Fig. 2e**) and a Parkinson's disease patient homozygous for the LRRK2 G2019S mutation (**Fig. 2f**). We found that increasing doses of LRRK2-IN-1 led to similar dephosphorylation of endogenous LRRK2 at Ser910 and Ser935 accompanied by loss of 14-3-3 binding, as was observed in HEK 293 cells stably expressing wild-type LRRK2 (compare **Fig. 2a** to **2e**) or LRRK2[G2019S] (compare **Fig. 2b** to **2f**). Moreover, endogenous LRRK2[G2019S] was also more sensitive to LRRK2-IN-1 than wild-type LRRK2 (compare **Fig. 2e** to **2f**). We also found that LRRK2-IN-1 induced a similar dose-dependent Ser910 and Ser935 dephosphorylation and loss of 14-3-3 binding to endogenous LRRK2 in human-derived neuroblastoma SHSY5Y cells (**Fig. 2g**) as well as mouse Swiss 3T3 cells (**Supplementary Fig. 7**).

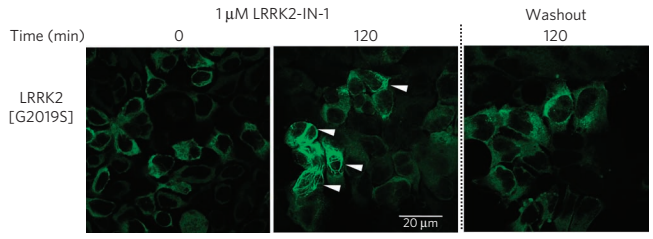

Figure 3 | LRRK2-IN-1 alters the cytoplasmic localization of LRRK2. HEK 293 cells stably expressing GFP-LRRK2[G2019S] were treated with 1 μM LRRK2-IN-1 for 2 h. Cells were then washed and fixed with 4% (w/v) paraformaldehyde for fluorescence imaging. To visualize LRRK2 localization after removal of LRRK2-IN-1, inhibitor-containing medium was removed 2 h after treatment. Cells were then washed twice and incubated with fresh medium without inhibitor for 2 h before again being washed and then fixed for fluorescence imaging. Representative micrographs of three independent experiments are presented.

LRRK2-IN-1 has favorable pharmacokinetics in mice with a half-life of 4.5 h, area under the curve of 14,758 h × ng ml^{-1} and bioavailability of 49.3% (**Supplementary Table 2**). After intraperitoneal injection of LRRK2-IN-1 into mice (100 mg kg^{-1}), we observed complete Ser910 and Ser935 dephosphorylation of LRRK2 in the kidney at the 1-h and 2-h time points (**Fig. 2h**). In contrast, no dephosphorylation of LRRK2 Ser910 or Ser935 was observed in the brain, indicating that LRRK2-IN-1 is likely unable to efficiently cross the blood-brain barrier (**Fig. 2h**).

Previous work suggested that dephosphorylation of Ser910 and Ser935 and loss of 14-3-3 binding promoted relocalization of LRRK2 to more aggregate and fibrillar-like structures[17] that might resemble inclusion bodies that certain mutant forms of LRRK2 have been reported to accumulate within[16,18,19]. To verify how LRRK2-IN-1 affected LRRK2 localization, we treated HEK293 cell lines stably expressing forms of full-length GFP-LRRK2 with 1 μM LRRK2-IN-1 over a 2-h time course. Prior to addition of LRRK2-IN-1, mutant LRRK2[G2019S] (**Fig. 3**) and wild-type LRRK2 (**Supplementary Fig. 8a**) were diffusely localized in the cytosol, consistent with previous work[17]. After addition of LRRK2-IN-1, we observed a significant accumulation of LRRK2[G2019S] (**Fig. 3**, **Supplementary Movie 1** and **Supplementary Fig. 9**) and wild-type LRRK2 (**Supplementary Fig. 8a** and **Supplementary Movie 2**) into aggregate structures. Notably, LRRK2-IN-1 did not affect the localization of drug-resistant LRRK2[A2016T] (**Supplementary Fig. 8b** and **Supplementary Movie 3**) or LRRK2[A2016T + G2019S] (**Supplementary Fig. 8c** and **Supplementary Movie 4**) mutants, which remained diffusely localized in the cytoplasm. Consistent with LRRK2 becoming rephosphorylated on Ser910 and Ser935 after inhibitor removal (**Supplementary Fig. 5**), LRRK2[G2019S] mutant (**Fig. 3** and **Supplementary Movie 2**) and wild-type LRRK2 (**Supplementary Fig. 8a** and **Supplementary Movie 1**) returned to a largely diffuse cytoplasmic relocalization within 2 h of LRRK2-IN-1 removal. LRRK1 does not bind 14-3-3, and the localization of LRRK1 does not change with LRRK2-IN-1 treatment (**Supplementary Fig. 10**).

In conclusion, we report upon the discovery of LRRK2-IN-1, to our knowledge the first selective and potent inhibitor of LRRK2. We establish that LRRK2-IN-1 rapidly suppresses LRRK2 kinase activity *in vivo* leading to dephosphorylation of Ser910 and Ser935, loss of 14-3-3 binding and accumulation of LRRK2 within aggregate fibrillar structures. LRRK2-IN-1 has the potential to transform our understanding of LRRK2 function, in the same way that other signal transduction inhibitors including PD98059 (ref. 20), SB203580 (ref. 21) and LY294002 (ref. 22) have aided with elucidation of the roles of Mek, p38 and PI 3-kinase, respectively. We recommend use of drug-resistant LRRK2[A2016T] mutant for validating that observed effects of LRRK2-IN-1 are indeed mediated via inhibition of LRRK2 kinase activity. LRRK2-IN-1 is a useful first-generation 'tool' compound and provides a starting point for developing a compound that could ultimately be used to address the potential therapeutic benefit of inhibiting LRRK2 in Parkinson's patients harboring the LRRK2 G2019S mutation.

Received 10 September 2010; accepted 29 January 2011; published online 6 March 2011

References

1. Gandhi, P.N., Chen, S.G. & Wilson-Delfosse, A.L. *J. Neurosci. Res.* **87**, 1283–1295 (2009).
2. Zimprich, A. *et al. Neuron* **44**, 601–607 (2004).
3. Paisán-Ruíz, C. *et al. Neuron* **44**, 595–600 (2004).
4. Healy, D.G. *et al. Lancet Neurol.* **7**, 583–590 (2008).
5. Dächsel, J.C. & Farrer, M.J. *Arch. Neurol.* **67**, 542–547 (2010).
6. Greggio, E. & Cookson, M.R. *ASN Neuro* **1**, e00002 (2009).
7. Covy, J.P. & Giasson, B.I. *Biochem. Biophys. Res. Commun.* **378**, 473–477 (2009).
8. Anand, V.S. *et al. FEBS J.* **276**, 466–478 (2009).
9. Nichols, R.J. *et al. Biochem. J.* **424**, 47–60 (2009).
10. Lee, B.D. *et al. Nat. Med.* **16**, 998–1000 (2010).
11. Goldstein, D.M., Gray, N.S. & Zarrinkar, P.P. *Nat. Rev. Drug Discov.* **7**, 391–397 (2008).
12. Fabian, M.A. *et al. Nat. Biotechnol.* **23**, 329–336 (2005).
13. Karaman, M.W. *et al. Nat. Biotechnol.* **26**, 127–132 (2008).
14. Bain, J. *et al. Biochem. J.* **408**, 297–315 (2007).
15. Patricelli, M.P. *et al. Biochemistry* **46**, 350–358 (2007).
16. Nichols, R.J. *et al. Biochem. J.* **430**, 393–404 (2010).
17. Dzamko, N. *et al. Biochem. J.* **430**, 405–413 (2010).
18. Alegre-Abarrategui, J. *et al. Hum. Mol. Genet.* **18**, 4022–4034 (2009).
19. Greggio, E. *et al. Neurobiol. Dis.* **23**, 329–341 (2006).
20. Alessi, D.R. *et al. J. Biol. Chem.* **270**, 27489–27494 (1995).
21. Cuenda, A. *et al. FEBS Lett.* **364**, 229–233 (1995).
22. Vlahos, C.J. *et al. J. Biol. Chem.* **269**, 5241–5248 (1994).

Acknowledgments

We wish to thank staff at the National Centre for Protein Kinase Profiling (http://www.kinase-screen.mrc.ac.uk) for undertaking Dundee kinase specificity screening, F. Hentati (Institut National de Neurologie, Tunisia) and A. Reith (GlaxoSmithKline Pharmaceuticals Research and Development) for providing EBV immortalized human lymphoblastoid cells, P. Bamborough (GlaxoSmithKline Pharmaceuticals Research and Development) for providing LRRK2 homology model and the antibody purification teams (Division of Signal Transduction Therapy (DSTT), University of Dundee) coordinated by H. McLauchlan and J. Hastie for generation of antibodies. This work was supported by US National Institutes of Health grant P41 GM079575-03 (N.S.G.), the Medical Research Council Technology Industry Collaboration Award and a National Health and Medical Research Council postdoctoral fellowship (N.D.), the Medical Research Council (D.R.A.), the Michael J. Fox Foundation for Parkinson's Disease Research (D.R.A.), the pharmaceutical companies supporting the DSTT (AstraZeneca, Boehringer-Ingelheim, GlaxoSmithKline, Merck KgaA and Pfizer) (D.R.A.), the US National Institutes of Health grants CA079871 and CA114059 (J.-D.L.) and funds from the Tobacco-Related Disease Research Program of the University of California, 19XT-0084, (J.-D.L.).

Author contributions

N.S.G. conceived and directed the chemistry effort. X.D. performed the chemical synthesis and structure-activity relationship analysis. D.R.A. conceived and directed the biology effort. N.D. performed the biology experimental research with assistance from A.P. (confocal microscopy and live cell imaging). P.D. performed the SHSY5Y experiment. Q.L. performed the modeling study. Q.Y. and J.-D.L. performed the MAPK7 cellular assay. M.P.P. and T.K.N. performed the KiNativ selectivity profiling and data analysis. X.D., N.D., D.R.A. and N.S.G. co-wrote the paper. All authors read and edited the manuscript.

Competing financial interests

The authors declare competing financial interests: details accompany the full-text HTML version of the paper at http://www.nature.com/naturechemicalbiology/.

Additional information

Supplementary information, chemical probe information and chemical compound information is available online at http://www.nature.com/naturechemicalbiology/. Reprints and permissions information is available online at http://npg.nature.com/reprintsandpermissions/. Correspondence and requests for materials should be addressed to D.R.A. or N.S.G.